

Finite difference modelling of the full acoustic wave equation in Matlab

Hugh D. Geiger and Pat F. Daley

ABSTRACT

Two subroutines have been added to the Matlab AFD (acoustic finite difference) package to permit acoustic wavefield modeling in variable density and variable velocity media. A centered finite difference scheme using a 5 point approximation has been chosen to closely approximate the full acoustic wave equation modeling used to generate the original Marmousi data set. Sampling of the wavefield in both time and space is an important consideration for accuracy, stability, and efficiency. A minimum of 10 spatial samples per wavelength and preferably 20 are required to eliminate phase and group velocity dispersion (commonly referred to as grid dispersion), while “Bording’s conjecture” can be applied to determine the time sampling interval required for stability. Given these considerations, we show that the original Marmousi dataset likely contains significant grid dispersion.

INTRODUCTION

Standard finite-difference methods for the scalar wave equation have been implemented as part of the CREWES Matlab toolbox by Youzwishen and Margrave (1999) and Margrave (2000). These implementations handle a variable-velocity subsurface and a variety of simple boundary conditions. An obvious extension is to incorporate variable density. There are two motivations for this work. Our primary motivation was to gain further insight into the Marmousi acoustic synthetic dataset. A secondary purpose was to create Matlab code suitable for generation of synthetic datasets.

The Marmousi dataset (Versteeg and Grau, 1991) was created using a second-order finite-difference scheme. We are currently using the Marmousi dataset to test prestack shot-record depth-migration imaging algorithms based on recursive Kirchhoff extrapolators (Geiger et al. 2003). Good imaging requires attention to a number of factors, including preprocessing of the data to zero-phase with maximum bandwidth and source modeling for forward wavefield extrapolation. In Marmousi, realistic source and receiver arrays combine with a free-surface and hard water bottom to create an unknown source wavelet. By duplicating the Marmousi waterbottom and simplifying the subsurface beneath to constant velocity, we can isolate the Marmousi shot wavelet as well as the shot array and ghosting effects that largely determine the directional amplitudes of the propagating source wavefield.

As is well known in the literature (e.g. Levander, 1989), standard finite differences are not ideal for generation of accurate synthetic acoustic wavefields. They suffer from grid dispersion and grid anisotropy. These effects can be reduced with a corresponding computational cost. Good overviews of stability and accuracy methods for standard finite-differences can be found in Bording and Lines (1997) and Carcione et al. (2002). Over the last two decades, alternatives to standard finite differences have been developed

that are significantly more accurate. A simple option is to introduce a more symmetric operator for the Laplacian in the scalar wave equation or its equivalent in the acoustic wave equation (Cole, 1994; Fomel and Claerbout, 1997). Even higher accuracy can be obtained with non-standard finite-difference schemes (Micken, 1984; Cole, 2000). Recently, CREWES researchers have focused on modeling of isotropic and anisotropic elastic media (Bale, 2002a; Manning and Margrave, 1999, 2002).

In this paper, we derive the standard finite-difference equations for the acoustic wave equation. A similar derivation can be found in Zakaria et al. (2000), and a more generalized treatment in course notes by Li (2002). We then look briefly at accuracy and stability, and show that the Marmousi data set suffers from grid dispersion. This is not a new result – it was noted by Versteeg in his PhD thesis on Marmousi (1991) as a necessary compromise in order to gain computational efficiency. It does suggest, however, that Marmousi might not be an ideal dataset for comparison of imaging algorithms, especially if the parameters governing preprocessing and shot modeling are not published along with the images.

2-D STANDARD FINITE-DIFFERENCE THEORY

The wave equation for acoustic pressure $\phi(\mathbf{x}, t)$ at position \mathbf{x} and time t is given by

$$\nabla \cdot \left(\frac{1}{\rho(\mathbf{x})} \nabla \phi(\mathbf{x}, t) \right) - \frac{1}{K(\mathbf{x})} \frac{\partial^2 \phi(\mathbf{x}, t)}{\partial t^2} = -\frac{\partial^2 i_v(\mathbf{x}, t)}{\partial t^2} + \nabla \cdot \left(\frac{1}{\rho(\mathbf{x})} \mathbf{f}_v(\mathbf{x}, t) \right), \quad (1)$$

where $\rho(\mathbf{x})$ is the static density, $K(\mathbf{x})$ is the adiabatic compression modulus, $\partial^2 i_v(\mathbf{x}, t)/\partial t^2$ represents a point source of volume injection per unit volume, and $\nabla \cdot ((1/\rho(\mathbf{x}))\mathbf{f}_v(\mathbf{x}, t))$ represents a point source of force per unit volume. Henceforth, we limit the discussion to the 2-D case where $\mathbf{x} = (x, z)$.

In most situations, we are interested in solving the homogeneous case where the source terms on the RHS of equation (1) are zero. Where a source is required, Wapenaar and Berkhout (1989) show that the first term on the RHS acts as a monopole, while the second term acts as a dipole that can be synthesized from the monopole response. A monopole is a useful physical source, representing, for example, the marine airguns in the Marmousi source arrays. For these reasons, we consider only the monopole source.

Ignoring the dipole source and multiplying through by density gives

$$\rho(\mathbf{x}) \nabla \cdot \left(\frac{1}{\rho(x, z)} \nabla \phi(x, z, t) \right) - \frac{1}{c(x, z)^2} \frac{\partial^2 \phi(x, z, t)}{\partial t^2} = -\rho(x, z) \frac{\partial^2 i(t)}{\partial t^2} \delta(\mathbf{x} - \mathbf{x}_s), \quad (2)$$

where $c = (K/\rho)^{1/2}$ is now the speed of wave propagation in the media (the acoustic velocity), and $\partial^2 i(t)/\partial t^2$ is the time derivative of the rate at which volume is added to the fluid outside some small fixed region enclosing the delta function source $\delta(\mathbf{x} - \mathbf{x}_s)$

located at \mathbf{x}_s . Equation (2) is a more useful form for finite difference derivation, given that the subsurface parameters are typically specified by spatially varying grids of velocity and density.

It is reasonably straightforward to implement equation (2) as a second-order finite-difference scheme. On a uniform 2D grid with coordinates $x_i = i\Delta x$ and $z_j = j\Delta z$, and time sampling $t^n = n\Delta t$ the acoustic pressure can be specified as $\phi = \phi(x, z, t) = \phi_{i,j}^n$ and the static density as $\rho = \rho(x, z) = \rho_{i,j}$. The time derivative is calculated as the standard second-order finite difference scheme:

$$\frac{\partial^2 \phi(t)}{\partial t^2} = \frac{\phi(t + \Delta t) - 2\phi(t) + \phi(t - \Delta t)}{\Delta t^2} = \frac{\phi^{n+1} - 2\phi^n + \phi^{n-1}}{\Delta t^2}. \quad (3)$$

In the homogeneous case, one can solve for the wavefield at time t^{n+1} by combining equations (2) and (3)

$$\phi^{n+1} = \Delta t^2 v_{i,j}^2 \rho_{i,j} \nabla \cdot \left(\frac{1}{\rho} \nabla \phi \right) + 2\phi^n - \phi^{n-1}. \quad (4)$$

Now all that remains is to consider the operator

$$\nabla \cdot \left(\frac{1}{\rho} \nabla \phi \right). \quad (5)$$

Equation (5) is the divergence of the vector field $\nabla \phi_{i,j}^n$ with variable coefficients $1/\rho_{i,j}$. The divergence can be calculated for the area surrounding the point (x_i, z_j) using second-order centered finite differences, with both the vector field and the variable coefficient specified at the boundaries of the area:

$$\begin{aligned} \nabla \cdot \left(\frac{1}{\rho} \nabla \phi \right) &= \left(\frac{\partial}{\partial x} \mathbf{i}, \frac{\partial}{\partial z} \mathbf{j} \right) \cdot \left(\frac{1}{\rho} \frac{\partial \phi}{\partial x} \mathbf{i}, \frac{1}{\rho} \frac{\partial \phi}{\partial z} \mathbf{j} \right) \\ &= \frac{\left(\left(\frac{1}{\rho} \right)_{i+1/2,j} \frac{\partial \phi_{i+1/2,j}^n}{\partial x} - \left(\frac{1}{\rho} \right)_{i-1/2,j} \frac{\partial \phi_{i-1/2,j}^n}{\partial x} \right)}{\Delta x} + \frac{\left(\left(\frac{1}{\rho} \right)_{i,j+1/2} \frac{\partial \phi_{i,j+1/2}^n}{\partial z} - \left(\frac{1}{\rho} \right)_{i,j-1/2} \frac{\partial \phi_{i,j-1/2}^n}{\partial z} \right)}{\Delta z}. \end{aligned} \quad (6)$$

The gradient of the pressure is now expanded as a centered finite difference:

$$\begin{aligned} \nabla \cdot \left(\frac{1}{\rho} \nabla \phi \right) &= \frac{\left(\left(\frac{1}{\rho} \right)_{i+1/2,j} \frac{(\phi_{i+1,j}^n - \phi_{i,j}^n)}{\Delta x} - \left(\frac{1}{\rho} \right)_{i-1/2,j} \frac{(\phi_{i,j}^n - \phi_{i-1,j}^n)}{\Delta x} \right)}{\Delta x} \\ &+ \frac{\left(\left(\frac{1}{\rho} \right)_{i,j+1/2} \frac{(\phi_{i,j+1}^n - \phi_{i,j}^n)}{\Delta z} - \left(\frac{1}{\rho} \right)_{i,j-1/2} \frac{(\phi_{i,j}^n - \phi_{i,j-1}^n)}{\Delta z} \right)}{\Delta z}, \end{aligned} \quad (7)$$

which can be rearranged to yield

$$\begin{aligned} \nabla \cdot \left(\frac{1}{\rho} \nabla \phi \right) &= \frac{(1/\rho)_{i+1/2,j} \phi_{i+1,j}^n - \left((1/\rho)_{i+1/2,j} + (1/\rho)_{i-1/2,j} \right) \phi_{i,j}^n + (1/\rho)_{i-1/2,j} \phi_{i-1,j}^n}{\Delta x^2} \\ &+ \frac{(1/\rho)_{i,j+1/2} \phi_{i,j+1}^n - \left((1/\rho)_{i,j+1/2} + (1/\rho)_{i,j-1/2} \right) \phi_{i,j}^n + (1/\rho)_{i,j-1/2} \phi_{i,j-1}^n}{\Delta z^2}. \end{aligned} \quad (8)$$

Equation (8) agrees with equation (7.14) of Zhilin Li's teaching notes (2002). If density is constant, equation (8) reduces to the standard second-order form for the Laplacian with weights (1,-2,1) in each spatial dimension. Equation (8) suggests that the finite-difference scheme for the divergence is of the same second-order form. Later, we use this observation to conclude that Bording's conjecture for stability of finite difference schemes for the scalar wave equation (Lines et al., 1999) applies equally well to the acoustic wave equation.

For variable density, the value of $(1/\rho)_{i+1/2,j}$ is calculated as the harmonic average of densities at adjacent points

$$\left(\frac{1}{\rho} \right)_{i+1/2,j} = \frac{1}{2} \left(\frac{1}{\rho_{i+1,j}} + \frac{1}{\rho_{i,j}} \right), \quad (9)$$

and similarly for $(1/\rho)_{i-1/2,j}$, $(1/\rho)_{i,j+1/2}$, and $(1/\rho)_{i,j-1/2}$.

A simple expressions for a finite-difference algorithm can be obtained by combining equations (7) and (9) with the additional $\rho_{i,j}$ term from equation (4), yielding

$$\begin{aligned} \rho_{i,j} \nabla \cdot \left(\frac{1}{\rho} \nabla \phi \right) &= \frac{1}{2\Delta x^2} \left[\frac{(\phi_{i+1,j}^n - \phi_{i,j}^n)(\rho_{i+1,j} + \rho_{i,j})}{\rho_{i+1,j}} - \frac{(\phi_{i,j}^n - \phi_{i-1,j}^n)(\rho_{i,j} + \rho_{i-1,j})}{\rho_{i-1,j}} \right] \\ &+ \frac{1}{2\Delta z^2} \left[\frac{(\phi_{i,j+1}^n - \phi_{i,j}^n)(\rho_{i,j+1} + \rho_{i,j})}{\rho_{i,j+1}} - \frac{(\phi_{i,j}^n - \phi_{i,j-1}^n)(\rho_{i,j} + \rho_{i,j-1})}{\rho_{i,j-1}} \right]. \end{aligned} \quad (10)$$

Equation (10) has been coded as matlab function 'ders2_5pt.m'.

The wavefield at time t^{n+1} is calculated by equation (4), repeated here with the ‘ders2_5pt.m’ term in square brackets:

$$\phi^{n+1} = \Delta t^2 v_{i,j}^2 \left[\rho_{i,j} \nabla \cdot \left(\frac{1}{\rho} \nabla \phi \right) \right] + 2\phi^n - \phi^{n-1} \quad (11)$$

Equation (11) has been coded as the matlab function ‘afd_snap_acoustic.m’.

The acoustic finite difference functions are designed to integrate with other functions and programs in the CREWES Matlab AFD toolbox ‘finitedif’ (Youzwishen and Margrave, 1999). The x and z grid spacing are assumed to be equal. The only additional parameter required is a grid of spatially-varying densities sampled at the same spacing as the velocity (and wavefield computation) grid. Given that reflectivity arises from impedance contrasts (the product of velocity and density), these additional routines can be used to create constant velocity or $v(z)$ synthetics with complicated subsurface reflectivity, just by creating sharp density contrasts at the desired location of the reflectors.

Boundary conditions are not investigated in detail in this study. A discussion on finite difference methods for reflecting and nonreflecting (absorbing) boundary conditions can be found in Bording and Lines (1997). The reflecting condition is the simplest, and often chosen to model a free surface (pressure release) at the upper boundary. A line of fictitious nodes are placed above the top of the model. These nodes are given initial values of zero and kept zero for all model times. A comparison of finite difference model results with analytic results suggests that this places the true effective free surface at node location $-\Delta z/2$, which can have a subtle but significant effect on traveltimes and amplitudes when compared against expected analytic results for ghosted source and receiver arrays (e.g. Marmousi). Youzwishen and Margrave (1999) implement absorbing boundary conditions for the scalar wave equation with the Matlab routine ‘afd_bc_outer.m’. We make the weak assumption of constant density at the boundary so that we can apply this routine to the variable density case.

ACCURACY AND STABILITY TESTS

To ensure accurate and stable finite-difference calculations, the general method is to choose spatial sampling to avoid grid dispersion, and then chose temporal sampling to avoid numerical instability (Kelly and Marfurt, 1990, Mufti, 1990, as discussed in Lines et al. 1999). Here, we look specifically at the parameters used to model the Marmousi dataset, with velocities varying between 1500m/s and 5500m/s and a spatial sampling interval of 4m.

Equations for phase and group velocity dispersion can be found in Levander (1989). These were coded in Matlab to produce Figures 1a and 1b. Using a maximum Marmousi velocity of $v = 5500\text{m/s}$, grid spacing $h = 4\text{m}$, and 2D stability criteria $v\Delta t/h \leq 1/\sqrt{2}$ suggests a time sampling of $\Delta t = 0.0005\text{s}$ for stability. Wavefield sampling is 6.25 grid samples per wavelength at 1500 m/s and 60Hz maximum frequency. These figures suggest that there is significant phase and grid velocity dispersion (commonly referred to

as grid dispersion) in the shallow portion of the Marmousi dataset, as noted by Versteeg (1991).

Figure 2 was generated using an impulse in a constant velocity medium (2000m/s) with an upper free surface. The finite difference responses are compared against the analytic response computed using 2D Green's functions for grid sampling of 4m, 2m, 1m, and 0.5m corresponding to wavefield sampling of 8, 17, 34, and 70 samples per wavelength at maximum frequency of 60Hz. There is noticeable grid dispersion at 8 samples per wavelength (Figure 2a), much less at 17 samples per wavelength (Figure 2b), and effectively none at 34 and 70 samples per wavelength (Figures 2c and 2d). Note that some of the time delay arises because the effective free-surface is at a depth of $-\Delta z/2$, a factor not taken into account with the analytic response. Applying these results to the Marmousi dataset, we suggest that a grid sampling of 1m (corresponding to 25 samples per wavelength at minimum velocity of $v = 1500\text{m/s}$ and maximum frequency of $f = 60\text{Hz}$) would produce much more accurate data.

In additional tests (not shown here), we compared our algorithm to Peter Mannings elastic finite difference code (Manning, 1999), run with an S-wave velocity of zero. For the simple synthetics tested, the results were almost identical.

In Figure 3, an original shot record from Marmousi (shot 41, Figure 3a), is compared with a shot record generated using the Matlab finite difference code (Figure 3b). Figure 3c shows a portion of the near offset trace. The match is reasonably good, but not exact, suggesting that our acoustic finite-difference algorithm is not identical to the one used to generate the original data. However, the match is sufficiently close that we have confidence that our modeled results of near surface Marmousi wavefields will provide insight into the selection of preprocessing parameters and guide accurate modeling of the shot wavefield (see companion paper by Geiger et al. 2003).

CONCLUSIONS

In this paper, we derived the standard finite-difference equations for the acoustic wave equation with variable velocity and density. The equations were coded into two Matlab functions for use with the CREWES Matlab AFD toolbox 'finitedif'. Our primary motivation was to gain further insight into the Marmousi acoustic synthetic dataset as an aid to accurate prestack wave-equation depth imaging. An analysis of stability and accuracy suggests that the Marmousi data suffers from grid dispersion, and that a more accurate dataset could be produced with a grid sampling of 1m, corresponding to ~ 25 samples per wavelength at the minimum velocity and maximum frequency. Although we were not able to duplicate the Marmousi results exactly, we are confident that the new finite difference code can be used to generate simple synthetics that duplicate the waterbottom and free-surface ghosting effects in the Marmousi dataset. These synthetics provide insight into the selection of preprocessing parameters and guide accurate modeling of the shot wavefield.

REFERENCES

- Alford, R.M., Kelly, K.R. and Boore, D.M., 1974, Accuracy of finite-difference modeling of the acoustic wave equation, *Geophysics*, **39**, 834-842.
- Bale, R.A. 2002a, Modelling 3D anisotropic elastic data using the pseudospectral approach: CREWES Research Report **14**.
- Bording, R.P. and Lines, L.R., 1997, Seismic modeling and imaging with the complete wave equation, SEG Course Notes N8.
- Bourgeois, A., Lailly, P., and Versteeg, R., 1991, The Marmousi model in Versteeg, R., and Grau, G., Eds., *The Marmousi Experience: Proc. of 1990 EAGE Workshop on practical aspects of seismic data inversion*. IFP/Technip.
- Carcione, J.M., Herman, G.C., and ten Kroode, A.P.E., 2002, Y2K review article: Seismic modeling: *Geophysics* **67** 1304-1325.
- Cole, J.B., 1994, A nearly exact second-order finite-difference time-domain wave propagation algorithm on a coarse grid, *Computers in Physics*, **8**, 730-734.
- Cole, J.B., 2000, Application of nonstandard finite differences to solve the wave equation and Maxwell's equations, in Mickens (ed) *Applications of nonstandard finite difference schemes*, World Scientific.
- Fomel, S., and Claerbout, J.F., 1997, Exploring three-dimensional implicit wavefield extrapolation with the helix transform: SEP-95, 43-60
- Geiger, H.D., Margrave, G.F., Liu, K., and Daley, P.F., 2003, Depth imaging using slowness-averaged Kirchhoff extrapolators, CREWES Research Report **15**.
- Kelly, K.R. and Marfurt, K.J., 1990, Numerical modeling of seismic wave propagation: Soc. Expl. Geophys.
- Li, Z., 2002, Course notes for MA584: Numerical Solution of Differential Equations: Finite difference methods: available at <http://www4.ncsu.edu/~zhilin/TEACHING/MA584/index.html>
- Levander, A.R., 1989, Finite difference forward modeling in seismology, in James, D.E. (ed), *The encyclopedia of solid earth sciences*, Van Nostrand Reinhold, 410-431.
- Lines, L.R., Slawinski, R. and Bording, R.P., 1999. Short note: A recipe for stability of finite-difference wave-equation computations, *Geophysics*, **64**, 967-969.
- Manning, P.M. and Margrave, G.F., 1999, Finite difference modeling, Fourier analysis, and stability: CREWES Research Report, **11**.
- Manning, P.M. and Margrave, G.F., 2002, Optimum projections for finite-difference transmitting boundaries: CREWES Research Report, **14**.
- Mickens, R.E., 1984, *Nonstandard finite difference models of differential equations*, World Scientific.
- Mufti, I.R. 1990, Large-scale three-dimensional seismic models and their interpretive significance: *Geophysics*, **55**, 1166-1182.
- Margrave, G.F., 2000, New seismic modeling facilities in Matlab, CREWES Research Report **12**.
- Versteeg, R.J., 1991, Analyse du probleme de la determination du modele de vitesse par l'imagerie sismique, PhD thesis IFP, Universite Paris IV.
- Versteeg, R. and Grau, G., Eds., 1991, *The Marmousi Experience: Proc. of 1990 EAGE Workshop on practical aspects of seismic data inversion*. IFP/Technip.
- Youzwishen, C.F. and Margrave, G.F., 1999. Finite difference modeling of acoustic waves in Matlab, CREWES Research Report **11**.
- Zakaria, A., Penrose, J. Thomas, F., and Wang, X., 2000, The two-dimensional numerical modeling of acoustic wave propagation in shallow water, Australian Acoust. Soc. Conf.

FIGURES

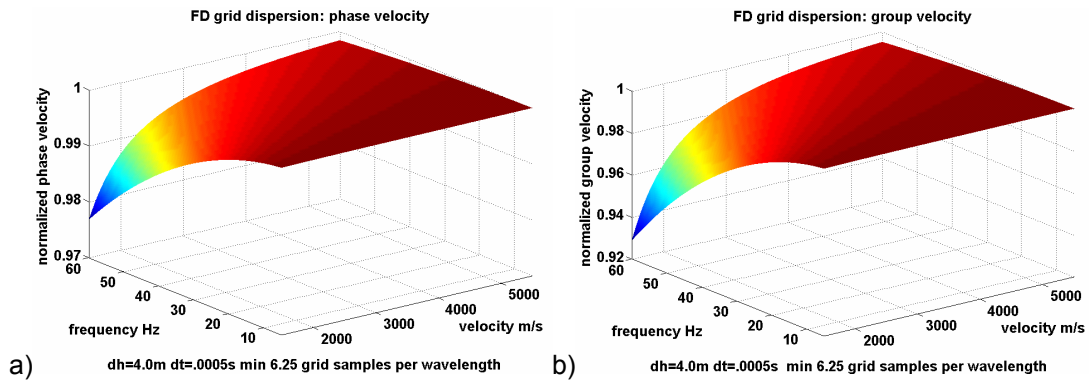


FIG. 1: Using maximum Marmousi velocity of $v = 5500\text{m/s}$, grid spacing $h = 4\text{m}$, and 2D stability criteria $v\Delta t/h \leq 1/\sqrt{2}$ suggests a time sampling of $\Delta t = 0.0005\text{s}$ for stability. Wavefield sampling is 6.25 grid samples per wavelength at 1500 m/s and 60Hz maximum frequency. Note the significant phase and grid velocity dispersion.

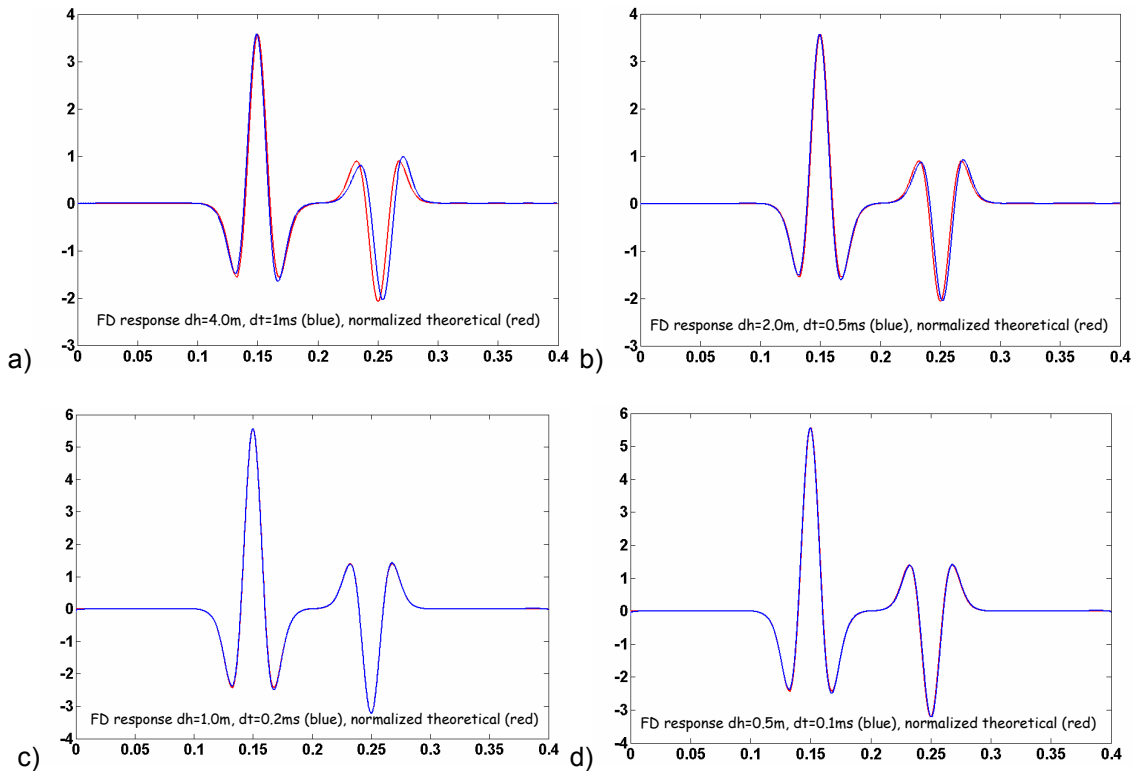


FIG. 2. The finite difference response in constant velocity medium (2000 m/s) for a direct and free-surface reflected wavelet with grid sampling of a) 4m (8 samples per wavelength), b) 2m (17), c) 1m (34) and d) 0.5m (70). The finite difference response (blue) overlies the ideal 2D analytic response (red). At 8 grid samples per wavelength, there is significant dispersion as the wavefield propagates. Some of the time delay is from the effective free-surface at $-\Delta z/2$, not accounted for in the analytic response. Grid sampling of ~ 20 samples per wavelength is recommended.

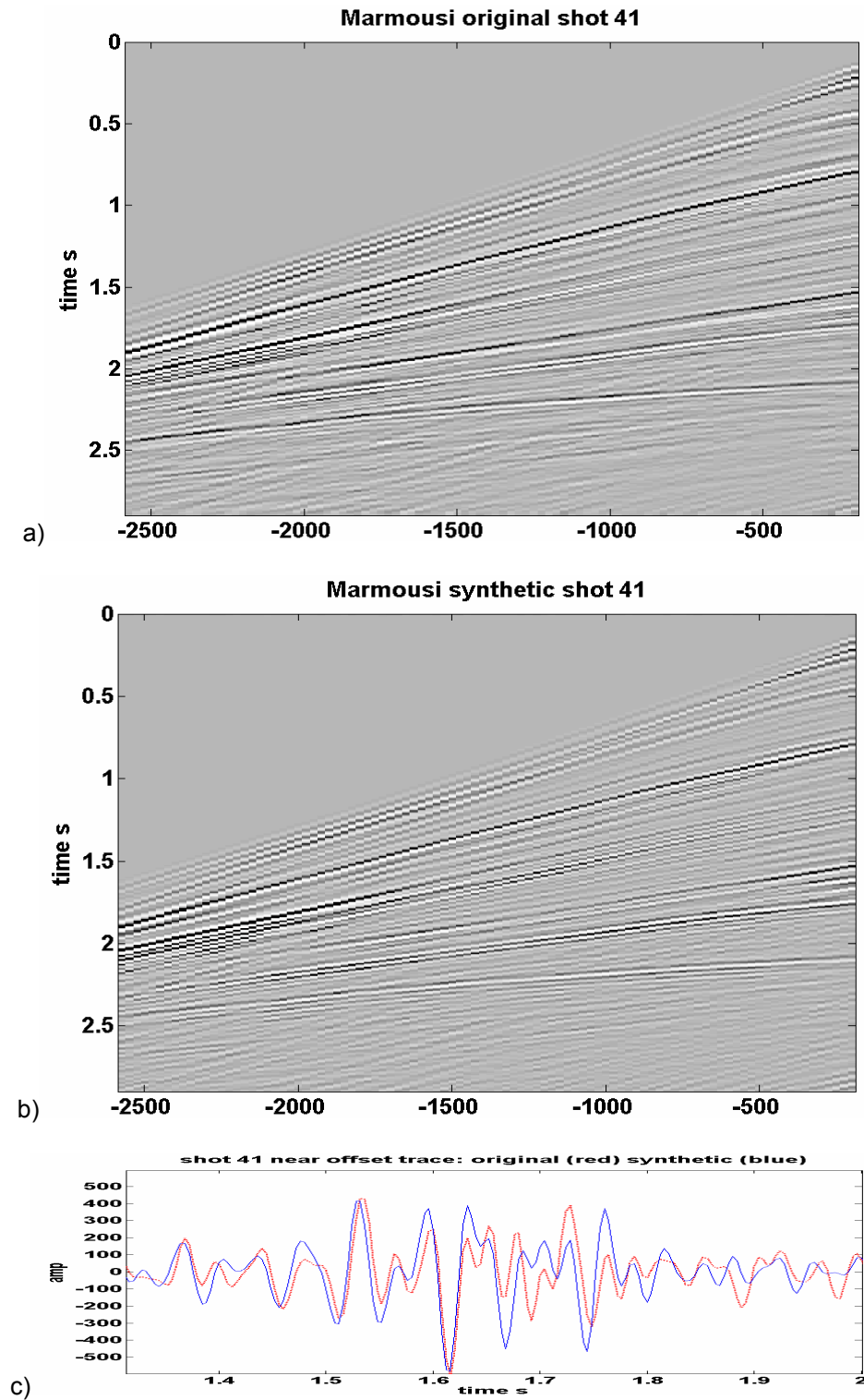


FIG 3. a) The original Marmousi data set for shot 41. b) Shot 41 generated using the Matlab finite difference routines for the acoustic wave equation. c) Portion of near trace showing that the match, although good, is not exact